Chemical Physics Letters 463 (2008) 289–299

Contents lists available at ScienceDirect

Chemical Physics Letters

journal homepage: www.elsevier.com/locate/cplett

FRONTIERS ARTICLE

Conical intersections and ultrafast intramolecular excited-state dynamics in nucleic acid bases and electron donor–acceptor molecules

Marek Z. Zgierski [a], Takashige Fujiwara [b], Edward C. Lim [b,*,1]

[a] Steacie Institute for Molecular Science, National Research Council of Canada, Ottawa, Canada K1A 0R6
[b] Department of Chemistry and The Center for Laser and Optical Spectroscopy, The University of Akron, Akron, OH 44325-3601, USA

ARTICLE INFO

Article history:
Received 16 May 2008
In final form 9 June 2008
Available online 13 June 2008

ABSTRACT

Conical intersections play important roles in photochemistry and photobiology through their preeminent control over the course of electronic relaxation processes. In this Letter, we present results from a combined experimental and computational study of ultrafast internal conversion in nucleic acid bases and intramolecular charge transfer in *N,N*-dialkylaminobenzonitriles, which indicate that these photoprocesses occur through three-state conical intersections involving an intermediate electronic state.

1. Introduction

Occurrence of intersection between molecular potential energy surfaces and their relevance to photophysics and photochemistry was recognized by Teller 70 years ago [1]. Nonadiabatic transitions from the upper to the lower energy surfaces normally occur at geometries where the two surfaces 'touch' each other (i.e., where they have the same energy). In the immediate vicinity of a touching point, the two surfaces are nearly degenerate, and a plot of the surface energies against two coordinates has the form of a double cone, i.e., conical intersection [2–5]. For a long time, it was believed that conical intersections (CI) occur mostly at energies high above the lowest-energy excited singlet (S_1) state, such that photophysics and photochemistry of molecules with low degrees of electronic excitation are not significantly affected by the intersections. This perception has changed rather dramatically in the 90s due to the advent of new experimental and theoretical methods. Theoretically, accurate multiconfigurational quantum theoretical methods, such as CASPT2//CASSCF (see Table 1 for a glossary of abbreviations and acronyms) [6–8], became available that can address nuclear geometries at the conical intersections and the way in which these intersections are accessed from the Franck–Condon region of the initially excited state. Experimentally, advances in femtosecond time-resolved laser spectroscopy (pump–probe and fluorescence upconversion, in particular) make it possible to probe, in real time, the ultrafast nonadiabatic passage from one electronic state to another that occurs through conical intersections [9–12]. The combination of these experimental and theoretical studies has yielded compelling evidence for the occurrence of low-energy conical intersections, and their central role in the spectroscopy and excited-state dynamics of polyatomic molecules.

The two especially important candidates for CI-controlled photoprocesses are the ultrafast internal conversion of photoexcited DNA/RNA bases [13], and the highly efficient intramolecular charge transfer (ICT) in dialkylaminobenzonitriles and related electron donor–acceptor (EDA) molecules [14]. Although these are two of the most extensively studied topics in physical chemistry and chemical physics during the past three decades, the reaction pathways for the nonadiabatic photodynamics have not been adequately identified or characterized until very recently. Using single reference ab initio and time-dependent DFT (TDDFT) methods, in combination with time-resolved laser spectroscopy, we have recently investigated the likely origins of the ultrafast energy and charge transfers in these molecular systems of fundamental importance to chemistry [15]. The results of this concerted theoretical and experimental study indicate that both the ultrafast radiationless decay (internal conversion) of photoexcited nucleobases and ultrafast ICT reaction of photoexcited dialkylaminobenzonitriles can be traced to the conical intersections of an intermediate electronic state with both the initially excited electronic state and the final electronic state. The final electronic state is the ground state for nucleobases and the ICT state for dialkylaminobenzonitriles. It is the purpose of this Letter to illustrate the importance of the three-state conical intersections in these two primary photoprocesses of very considerable importance. The paper is divided into three sections. The first describes the internal conversion of photoexcited DNA/RNA bases, and the second deals with the photoinduced intramolecular charge transfer in dialkylaminobenzonitriles (DMABN) and related electron donor-acceptor (EDA) molecules. The final section presents assessment of the reliability of the simple computational methods we have used to characterize the photodynamics of the two molecular systems.

* Corresponding author. Fax: +1 330 972 6407.
E-mail address: elim@uakron.edu (E.C. Lim).
[1] Holder of Goodyear Chair in Chemistry.

0009-2614/$ - see front matter © 2008 Elsevier B.V. All rights reserved.
doi:10.1016/j.cplett.2008.06.024

Table 1
Glossary of abbreviations and acronyms

ABN	Aminobenzonitrile
B3LYP	Becke three-parameter (B3) exchange functional with Lee, Yang, and Parr (LYP) correlation functional
CASPT2	Complete active space second-order perturbation theory
CASPT2//CASSCF	CASPT2 energy calculation at a geometry optimized with CASSCF
CASSCF	Complete active space self-consistent-field
CC	Coupled-cluster
cc-pVDZ	Correlation consistent, polarized valence double-zeta basis set
CCSD(T)	CC with singles, doubles, and perturbative triples
CI	Configuration interaction
CIS	CI with singles
CR-EOM-CCSD(T)	Completely renormalized Equation of motion CCSD(T)
DIABN	Diisopropylaminobenzonitrile
DMABN	Dimethylaminobenzonitrile
DMAPA	Dimethylaminophenylacetylene
EDA	Electron donor–acceptor
EOM-CCSD	Equation of motion coupled-cluster with singles and doubles
ICT	Intramolecular charge transfer
MRCI	Multireference CI
PdG	Propanodeoxyguanosine
PICT	Planar ICT
TDDFT	Time-dependent density functional theory
TICT	Twisted ICT
TMC	5,6-Trimethylenecytosine
TMU	5,6-Trimethyleneuracil

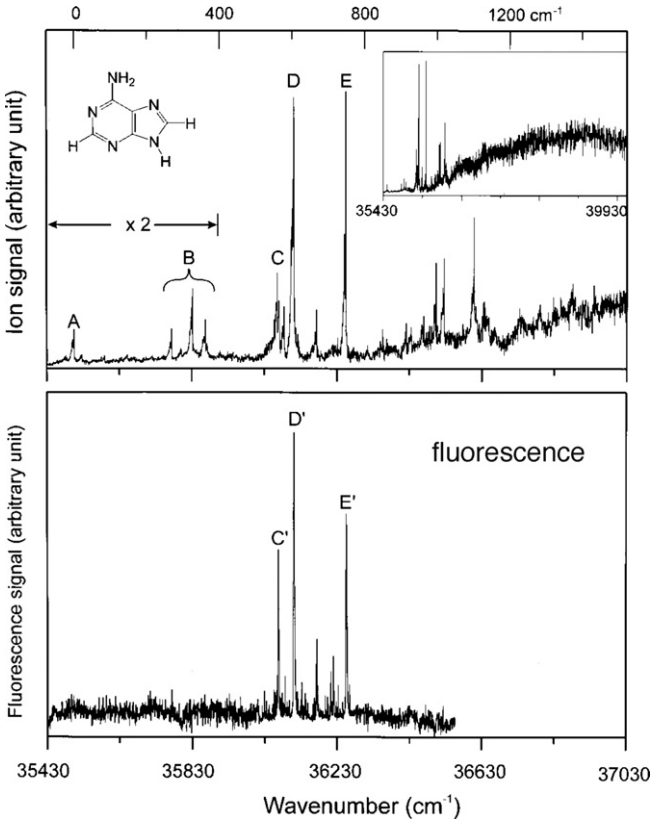

Fig. 1. Composite one-color resonant two-photon ionization (R2PI) spectrum of adenine (upper panel). Peak A is the origin band of the $n\pi^*$ transition, while peak D was assigned to the origin band of the $\pi\pi^*$ transition. The wavenumber scale on the top is relative to the 0–0 band of the $n\pi^*$ state. Starting from ~800 cm^{-1} above the 0–0 band, there appears a broad background underneath the sharp vibronic features. Fluorescence excitation spectrum of adenine (lower panel). The peaks denoted as C′, D′, and E′, respectively, correspond to the R2PI peaks C, D, and E in the above R2PI spectrum. (Reprinted with permission from Ref. [21].)

2. Ultrafast internal conversion of nucleic acid bases

Because of their biological importance, nucleic acid bases have been the subjects of many spectroscopic and photophysical studies over the past three decades [13]. The most striking photophysical property of the nucleobases is the extremely short excited-state (S_1) lifetime, caused by ultrafast radiationless decay (internal conversion) to the ground state (S_0). It is generally recognized that the highly efficient internal conversion of nucleic acid components provides DNA with a high degree of intrinsic photostability. In solution at room temperature, the excited-state (S_1) lifetimes of nucleobases, as measured by femtosecond transient absorption and fluorescence upconversion, are typically subpicosecond. The subpicosecond internal conversion (viz. S_1 lifetime) is too fast to be due to conventional radiationless transitions in which the photoexcited molecule tunnels from the adiabatic potential-energy surface (PES) of the excited state to that of the ground state (S_0) [16–19]. Instead, the subpicosecond decay is a characteristic feature of nonadiabatic photodynamics that occurs via surface crossing, i.e., CI.

The clearest experimental evidence for the involvement of a CI comes from the dramatic temperature dependence of S_1 lifetime in condensed phases [20] and the remarkable excitation energy dependence of S_1 lifetime under collision-free conditions of gas phase [21,22]. Specifically, the subpicosecond lifetimes of most bases in solution at room temperature increase to nanoseconds in glassy matrices at or below 77 K [20]. In the gas phase under supersonic expansion conditions, the fluorescence lifetimes of adenine [21] and guanine [22], which are in the range of nanoseconds

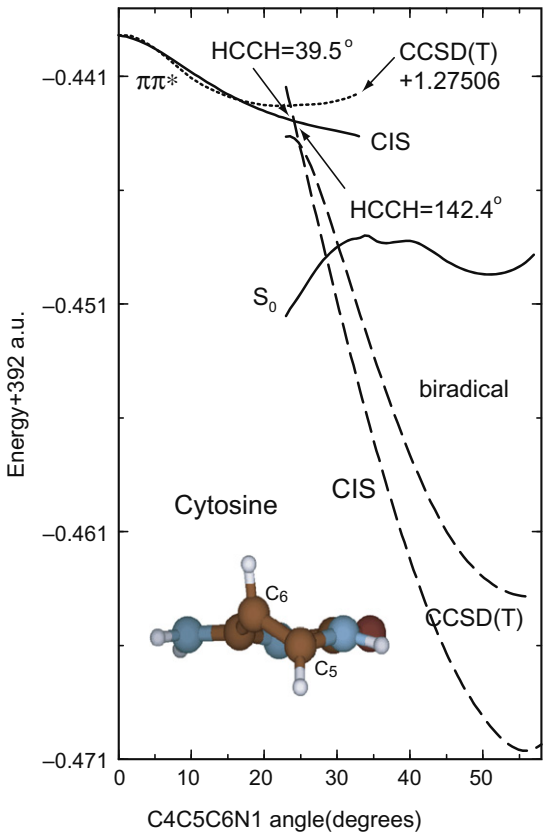

Fig. 2. The potential-energy profiles of the S_1 state of cytosine as a function of the C4C5C6N1 dihedral angle. EOM-CCSD(T) values are shifted uniformly upward by the amount indicated in the figure. The insert shows the side view of the minimum-energy structure of the biradical state. (Reprinted with permission from Refs. [23,25].)

for excitation into the very low-lying vibronic levels of the lowest-energy $\pi\pi^*$ state, decrease to subpicoseconds for excitation into the higher-lying vibronic levels. This leads to an abrupt break-off of fluorescence, which in adenine occurs at about 200 cm^{-1} above the electronic origin of the $^1\pi\pi^*$ state, Fig. 1. Both the anomalously strong temperature dependence of fluorescence in solution and the fluorescence break-off in supersonic free jets could be rationalized if a dark electronic state crosses the $\pi\pi^*$ state at energies slightly above the electronic origin of the $\pi\pi^*$ state.

To probe the possible existence of such a dark state, we have carried out CIS, CC2 and CCSD(T) calculations of the potential energy profiles for pyrimidine bases (cytosine [23], uracil [23], and thymine [24]) and their derivatives at optimized CIS geometries. The results indicate that the $S_1(\pi\pi^*) \rightarrow S_0$ internal conversion occurs through a low-barrier (or barrierless) state switch from the initially excited $^1\pi\pi^*$ to a biradical state, which in turn intersects the ground state at lower energy, Fig. 2. In the biradical state, the C5 and C6 hydrogen atoms (C5 methyl group and C6 hydrogen atom in thymine) are almost perpendicular to the average ring plane and are displaced in opposite directions (see inset of Fig. 2). As a result, the p_z orbitals of the C5 and C6 carbon atoms are decoupled from the π-electron system and are singly occupied, giving the state a biradical character. Significantly, the biradical-mediated internal conversion, deduced from the modest levels of theory, predicts that fluorination of the C5 hydrogen of cytosine or uracil (see Scheme 1 for structures and atom numbering) introduces a significant energy barrier for the $\pi\pi^* \rightarrow$ biradical state switch, whereas replacement of the C6 hydrogen has an opposite effect [25], Fig. 3. These predictions are borne out by the much longer S_1 lifetime of 5-fluorocytosine (~73 ps in aqueous solution at room temperature) [26] and the significantly shorter lifetime of 6-fluorocytosine (<0.25 ps) [25] relative to cytosine (0.72–0.76 ps) [26]. The biradical decay mechanism involving three-state conical intersections also predicts that the acetylation of the amino group attached to the C4 carbon atom of cytosine (see Scheme 1 for structure) greatly lengthens the S_1 lifetime by stabilizing the $^1\pi\pi^*$ state relative to the biradical state [23], Fig. 4. This prediction is supported by the remarkably long S_1 lifetime of N^4-acetylcytosine (~280 ps) [27,28]. It is interesting that the barrier height for the $\pi\pi^* \rightarrow$ biradical state switch is significantly smaller in uracil than in cytosine [29], Fig. 5, consistent with the much shorter S_1 lifetime of uracil (~0.1 ps in aqueous solution) [30,31] relative to that of cytosine.

More recently, we have performed CC2, EOM-CCSD and CR-EOM-CCSD(T) calculations of the potential energy profiles of the purine bases, adenine [32], and guanine [33] at optimized CIS geometries using the cc-pVDZ basis set. The results of this study indicate that the internal conversion of purine bases is also

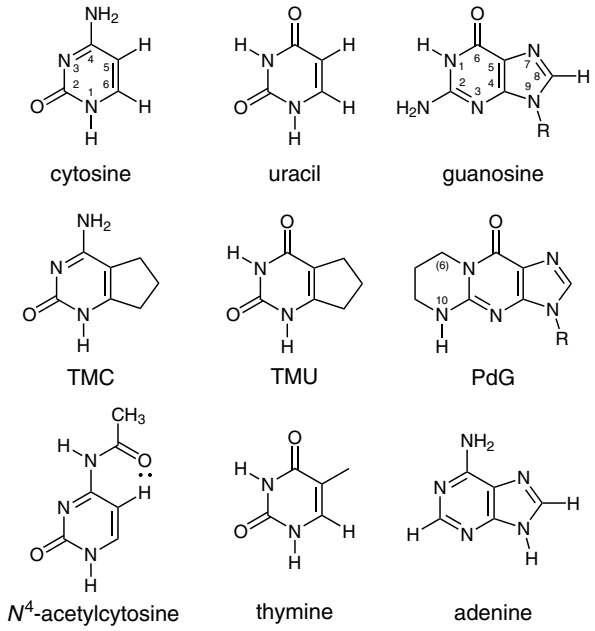

Scheme 1.

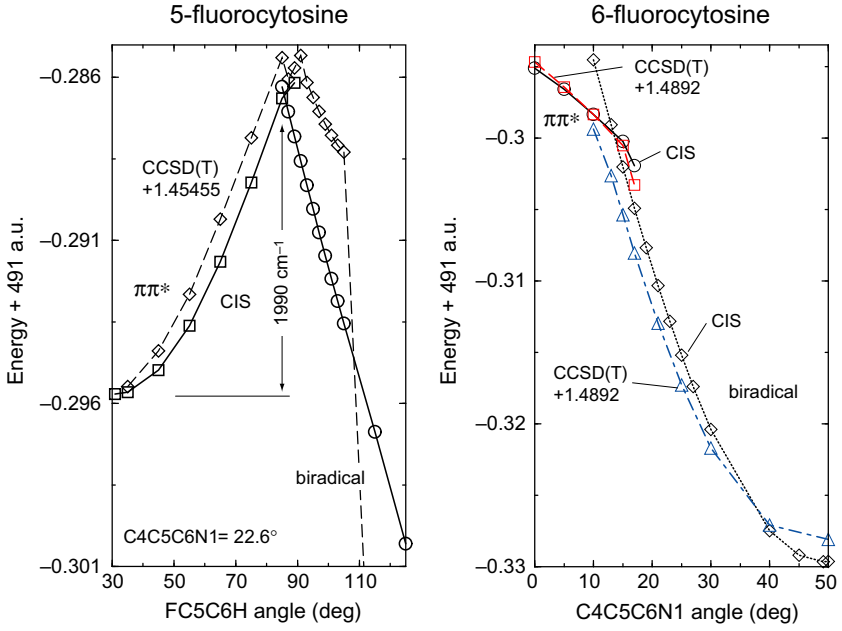

Fig. 3. The crossing of the $^1\pi\pi^*$ and biradical states in 5-fluorocytosine (left) and 6-fluorocytosine (right). For the 5-fluorocytosine, the squares and the circles represent the CIS energies of the $^1\pi\pi^*$ state and biradial state, respectively, and the diamonds denote the CCSD(T) $^1\pi\pi^*$ energies shifted by 1.45455 a.u. For the 6-fluorocytosine, the circles (CIS) and the squares (CCSD(T)) are the $^1\pi\pi^*$ state energies, whereas the diamonds (CIS) and the triangles (CCSD(T)) are the energies of the biradical state. The CCSD(T) energies are shifted by 1.4892 a.u. (Reprinted with permission from Refs. [23,25].)

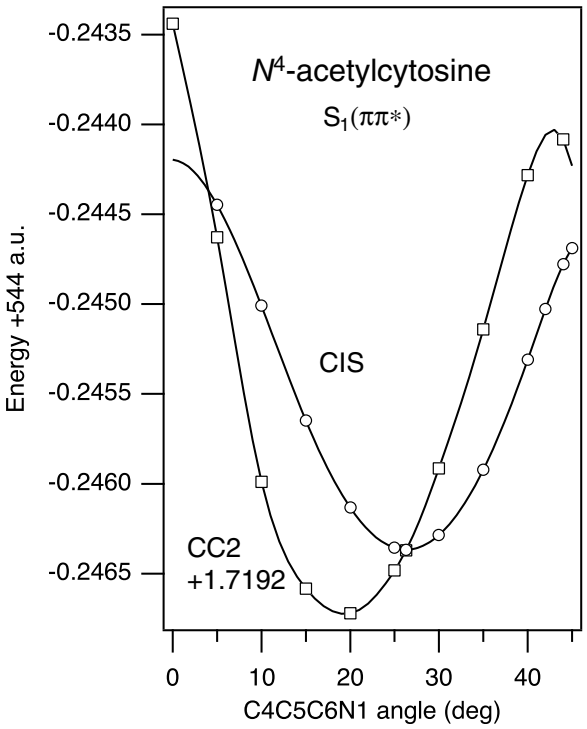

Fig. 4. CIS/cc-pVDZ and CC2/cc-pVDZ potential-energy profiles of the lowest-energy $^1\pi\pi^*$ state of N^4-acetylcytosine as a function of C4C5C6N1 dihedral angle. (Reprinted with permission from Ref. [15].)

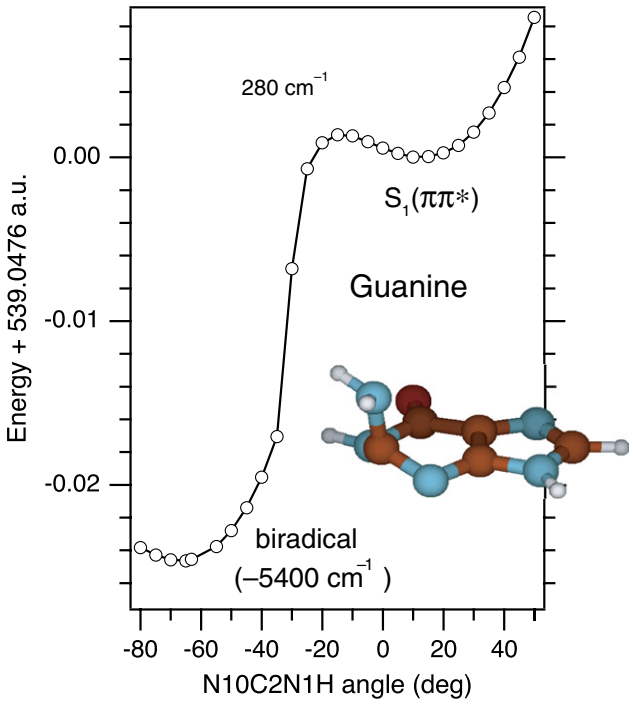

Fig. 6. CC2/cc-pVDZ potential-energy profiles of the $^1\pi\pi^*$ and biradical states of guanine as a function of N10C2N1H dihedral of angle. (Reprinted with permission from Ref. [42].)

mediated by a biradical state, which arises from the $\pi\pi^*$ state upon out-of-plane deformation of the pyrimidine ring, Fig. 6. The biradical state is characterized by an electronic configuration in which one unpaired electron occupies a π^* orbital localized on the five-membered ring and the other occupies an orbital localized very strongly on a p-type C2 atomic orbital of the six-membered ring [32,33]. Structurally, it has a strongly puckered six-membered ring and the C2–H bond (for adenine), or the C2–N bond (for guanine), which is nearly perpendicular to the average ring plane, as would result from the twist of the N3–C2 bond, Fig. 6. Consistent with the biradical-mediated radiationless decay, the measured $\pi\pi^*$-state lifetime in supersonic jets is extremely short (sub-picoseconds) in adenine and 9-methyladenine [34], which have the biradical state below the initially excited $\pi\pi^*$ state [32], slightly longer in *N*,*N*-dimethyladenine (~3 ps in gas phase) [34], which has a small energy barrier for the $\pi\pi^* \rightarrow$ biradical state switch, and much longer

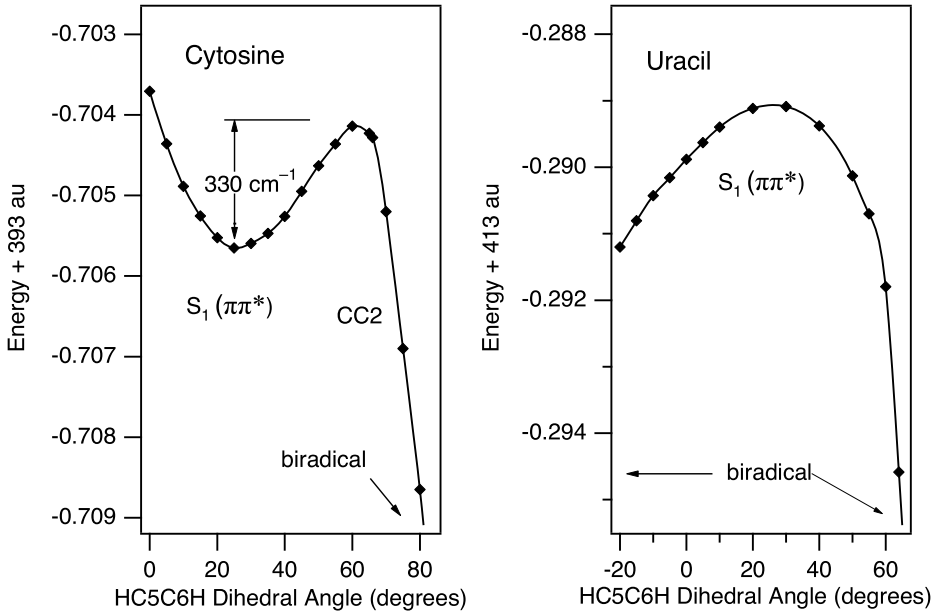

Fig. 5. CC2/cc-pVDZ potential-energy profiles of the $^1\pi\pi^*$ and biradical states of cytosine and uracil as a function of HC5C6H dihedral angle. The number (330 cm^{-1}) for cytosine refers to the energy barrier for the state switch from the $\pi\pi^*$ minimum to the biradical state. The dihedral angle at the ground-state minimum is 0°. (Reprinted with permission from Ref. [29].)

in 2-aminopurine [34], which has the biradical state substantially above the $\pi\pi^*$ state [32].

Interestingly, the biradical structures obtained from the geometry optimization with the simple CIS method are similar to the geometries at the $\pi\pi^*/S_0$ conical intersections (CI), for pyrimidines [31,35–37] and purines [38–41], located by using high-level multireference ab initio methods. This similarity suggests that the out-of-plane deformation leading to the $\pi\pi^*/S_0$ CI is closely related to the reaction pathway for isomerization of the planar $\pi\pi^*$-state geometry into the biradical geometry. It is possible that the low-level CIS method yields geometries very similar to those from the highly correlated methods due to the HOMO–LUMO character of the state involved (vide infra). Independent of the question of whether the CI with the ground state is accessed directly from the initially excited state or through an intermediate biradical state, it is expected that covalent modification of nucleic acid bases leading to hindrance of the C5–C6 twist in the pyrimidines and N3–C2 twist in the purines would lead to a dramatic retardation of the internal conversion rate. The predicted, critical role of the out-of-plane deformations could be tested experimentally by making use of tailor-made derivatives of nucleic acid bases in which the nonplanar deformation cannot easily occur due to steric constraints. To this end, we have recently synthesized and characterized the photophysical properties of 5,6-trimethylenecytosine (TMC) [29], 5,6-trimethyleneuracil (TMU) [29], and propanodeoxyguanosine (PdG) [42], Fig. 7. Consistent with expectation, the covalently modified nucleobases are strongly fluorescent compounds [29,42], Fig. 7. Fluorescence decay measurements, based on the picosecond time-correlated single-photon counting yield the lifetime of about 1.2 ns for TMC [29] about 29 ps for TMU [29]

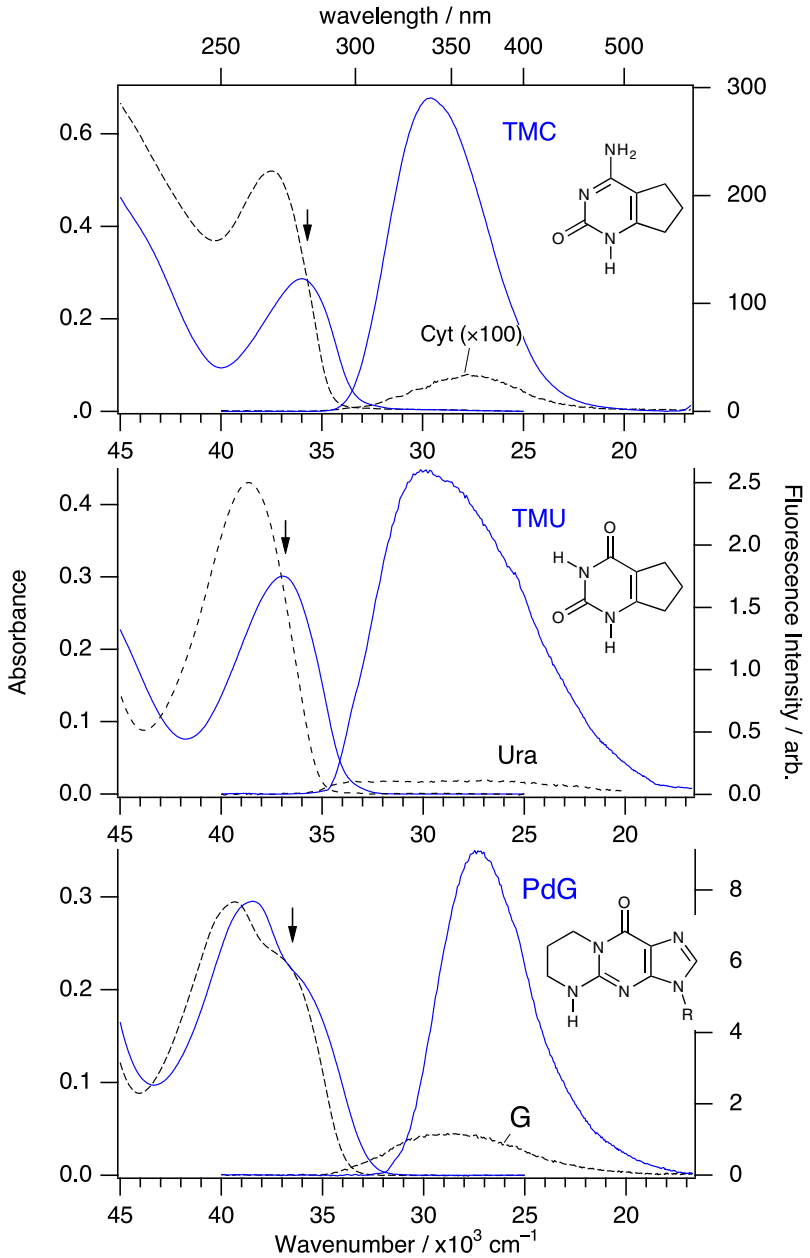

Fig. 7. Steady-state absorption and fluorescence spectra of (a) 5,6-trimethylenecytosine (TMC) and cytosine (Cyt), (b) 5,6-trimethyleneuracil (TMU) and uracil (Ura), and (c) propanodeoxyguanosine (PdG) and guanosine (G) in aqueous solutions of pH 7 at 25 °C. The steady-state fluorescence spectra of the two closely related compounds (natural and covalently-modified) in each panel were measured using solutions having the same absorbance (*ca.* 0.3) at the wavelength of excitation indicated by the arrow. (Adapted with permission from Refs. [29,42].)

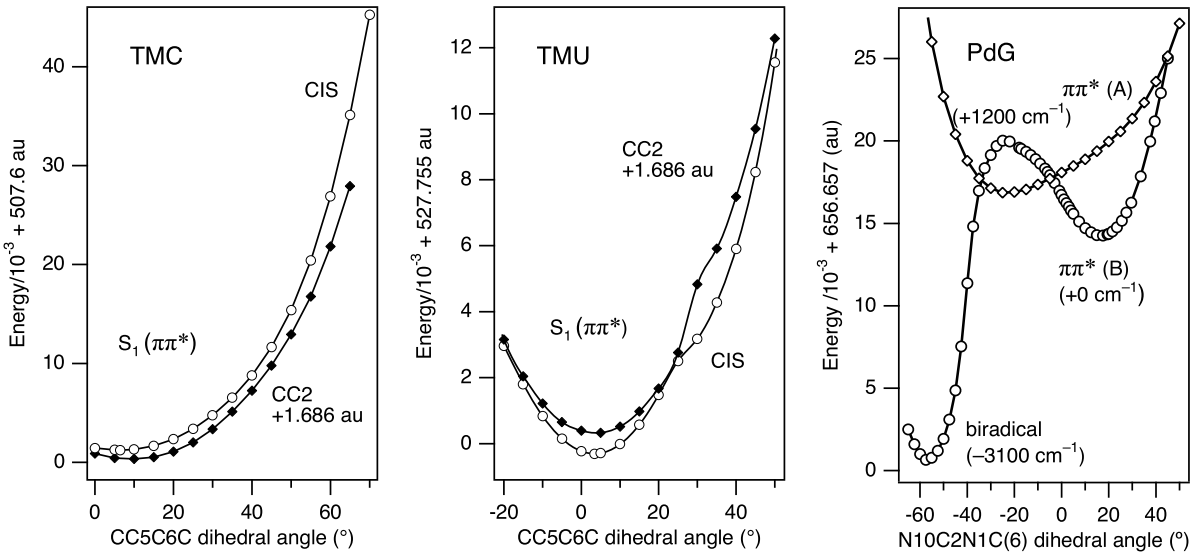

Fig. 8. CIS and CC2/cc-pVDZ potential-energy profiles of the $^1\pi\pi^*$ and biradical states for TMC (left) and TMU (middle) as a function of HC_5C_6H dihedral angle, and CC2/cc-pVDZ potential-energy profile of the $^1\pi\pi^*$ state for PdG (right) as function of N10C2N1C(6) dihedral angle. The conformer B of PdG leads to biradical state whereas the conformer A does not. Each dihedral angle at the ground-state minimum is referred to as 0°. (Reprinted with permission from Refs. [29,42].)

and about 12 ns for the slow-decaying component (assigned to a planar conformer) of PdG [42], in aqueous solution of pH 7 at room temperature. In conformity with these experimental results, coupled-cluster calculations indicate that the $^1\pi\pi^*$ state of TMC [29], TMU [29], and the planar conformer of PdG [42] all have $^1\pi\pi^*$ states that are very stable against the out-of-plane deformation (leading to biradical geometries) as shown in Fig. 8. The computed energetics also suggest that the dramatically shorter fluorescence lifetime of TMU relative to TMC can be attributed to the presence in TMU of an efficient, secondary nonradiative decay channel of the $\pi\pi^*$ state involving a close-lying $n\pi^*$ state [29] (as opposed to the TMC in which the $\pi\pi^*$ state is significantly below the $n\pi^*$ state).

3. Intramolecular charge transfer in 4-dialkylaminobenzonitriles

Intramolecular charge transfer (ICT) in electron donor–acceptor (EDA) molecules has long been a topic of great interest in photochemistry [14]. 4-Dimethylaminobenzonitrile (4-DMABN) is a prototype of EDA molecules that exhibit dual fluorescence, related to ICT, in polar solvents [43], Fig. 9. The shorter-wavelength emission with a small Stokes shift was assigned to the normal fluorescence from the lowest-energy $\pi\pi^*$ state (L_b), whereas the 'anomalous' longer-wavelength emission was attributed to the fluorescence from a highly polar, L_a-like charge-transfer (CT) state [43]. Consistent with the latter assignment, the picosecond transient absorption (TA) spectra of 4-DMABN in polar solvents display strong 320 nm and weaker 410 nm transients that closely mimic absorption spectra of benzonitrile anion [44]. A large number of subsequent studies have shown that the dual fluorescence is rather common among aminobenzonitriles and amino phenyl carbonyls [14].

The first proposal concerning the molecular structure of the emitting ICT state of 4-DMABN was made by Grabowski and coworkers [14,45,46]. In their model, commonly known as TICT (T for twisted), charge transfer from the dimethyl group to the benzonitrile moiety occurs in concert with the 90° twisting of the amino group with respect to the benzonitrile moiety. Since the driving force for the twisting is the minimization of the Coulomb interaction between the unpaired electrons, the TICT is an elegant and very reasonable model that is consistent with the principle of minimum overlap [46,47]. Although the TICT model had been challenged from time to time, especially by the alternative PICT (P for planar) model [48,49], almost all theoretical studies (quantum

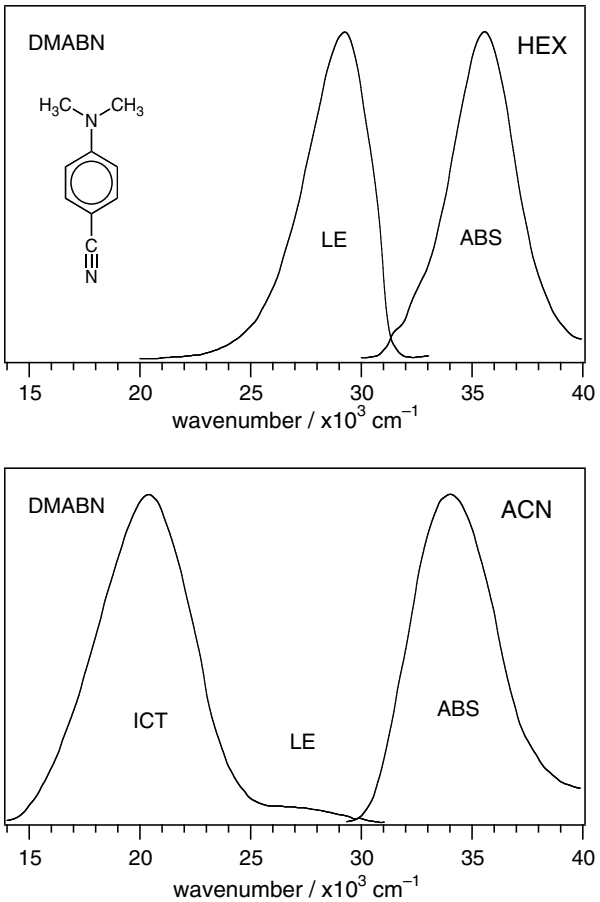

Fig. 9. Fluorescence and absorption spectra of 4-(dimethylamino)benzonitrile (4-DMABN) in acetonitrile (ACN) and in *n*-hexane (HEX) at 25 °C (Adapted with permission from Ref. [54].)

chemical calculations) [50] support the amino group twists as the reaction coordinate along which the ICT occurs. N–C_{phenyl} bond has a single bond character in the TICT structure and a double bond character in the PICT model. Picosecond infrared and Raman measurements [51] have shown that the N–C_{phenyl} bond has a single bond character, consistent with the TICT model. Further experimental support for the TICT model comes from the observation of only the ICT emission from the alkylaminobenzonitriles with pre-twisted amino group (3,5-dimethyl-4-DMABN, for example) [14] and the very interesting NMR study of unsymmetric analog of 4-DMABN [52], which demonstrates the twist of the amino group as the primary ICT reaction coordinate. It should be noted in this connection that the observation of the ICT emission in 'planarized' aminobenzonitrile, 1-*tert*-butyl-1,2,3,4-tetrahydroquinoline (NTC6) [49], is not a compelling support for the PICT model, as the six-membered exocyclic ring in the 'planarized' aminobenzonitrile may not be rigid [50], as the proponents of the PICT model assume. In fact, the covalently modified guanine, PdG, which has an exocyclic ring very similar to that in NTC6, exhibits dual fluorescence that most likely arises from the planar and twisted conformers [42], (see Fig. 7).

Most, if not all, experimental studies of the ICT reaction in solution begin with the excitation of the highly allowed $L_a \leftarrow S_0$ absorption [53,54]. The electronically excited molecules in the L_a state then very rapidly relax to the fluorescent L_b state, often referred to as locally excited (LE) state. Analysis of the biexponential decays of the LE and ICT fluorescence from 4-DMABN in polar solvents, shows that the rise (formation) time of the ICT emission is identical to the lifetime of the fast decaying component of the LE emission, indicating that the ICT state of 4-DMABN is formed directly from the LE state [53]. The LE → ICT reaction mechanism would be entirely reasonable, if not for the complication that the $\pi\pi^*$ (L_b and L_a) states are not the only low-lying excited electronic states of the molecule.

Recent studies of Sobolewski and Domcke [55–57], and our own [15,58], have revealed the existence of a low-lying excited state of $\pi\sigma^*$ configuration, which arises from the promotion of an electron from the aromatic π orbital to the σ^* orbital localized on the cyano group. Our TDDFT/cc-pVDZ and CIS/cc-pVDZ calculations on 4-DMABN and 4-aminobenzonitrile (4-ABN) indicate that the lowest-energy $\pi\sigma^*$ state of bent geometry (with C–C–N angle of about 120°) is in fact lower in energy than the lowest-energy $\pi\pi^*$ state of L_b type, at their respective optimized geometries [58], Fig. 10. Because the vertical transition from the ground state of linear geometry to the $\pi\sigma^*$ state of bent geometry is Franck–Condon forbidden, direct excitation of the ground-state molecule to the $\pi\sigma^*$ is not allowed, and the radiative transition from the $\pi\sigma^*$ state to the ground state is essentially dipole forbidden. The $\pi\sigma^*$ state is therefore a dark state that is formed, and decays, by radiationless transitions. At the optimized ground-state geometry, the vertical excitation energy of the dark $\pi\sigma^*$ state of 4-DMABN or 4-ABN is greater than that of the $\pi\pi^*$ state, and the two states cross at C–C–N angle of about 150° [58]. The energy barrier for the state crossing from the potential energy minimum of $\pi\pi^*$ state (L_b or L_a) to the dark $\pi\sigma^*$ state is less than 0.2 eV. The predicted state switch from the initially excited $\pi\pi^*$ state to the dark $\pi\sigma^*$ state is supported by

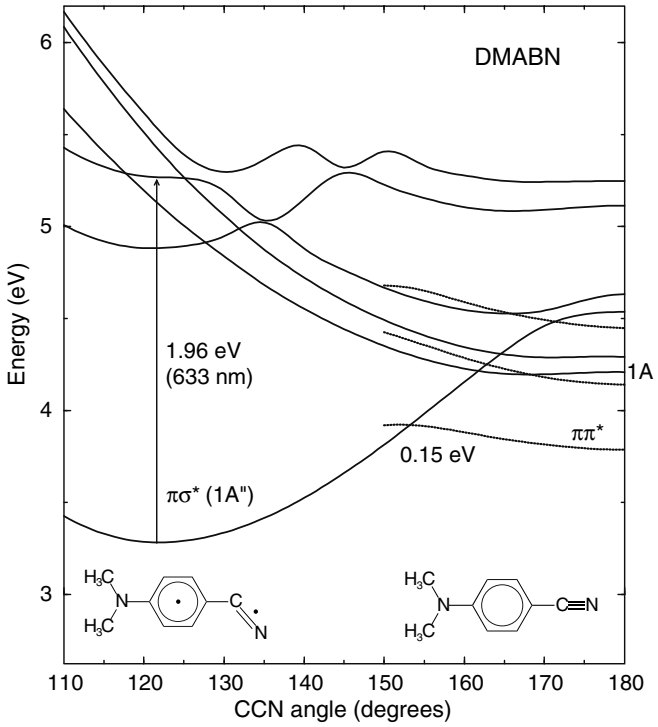

Fig. 10. TDDFT energies of low-lying excited singlet states of 4-DMABN as a function of C_{Ph}–C–N angle, as calculated using TD/BP86/6-311++G** level of theory. The solid curves are for the optimized CIS/6-311++G** geometries of the $\pi\sigma^*$ state, whereas the dotted curves are for the corresponding optimized $\pi\pi^*$ states in which the dimethylamino group is rotated and tilted. The vertical arrow denotes the highly allowed $\pi\sigma^* \leftarrow \pi\sigma^*$ transition. (Reprinted with permission from Ref. [58].)

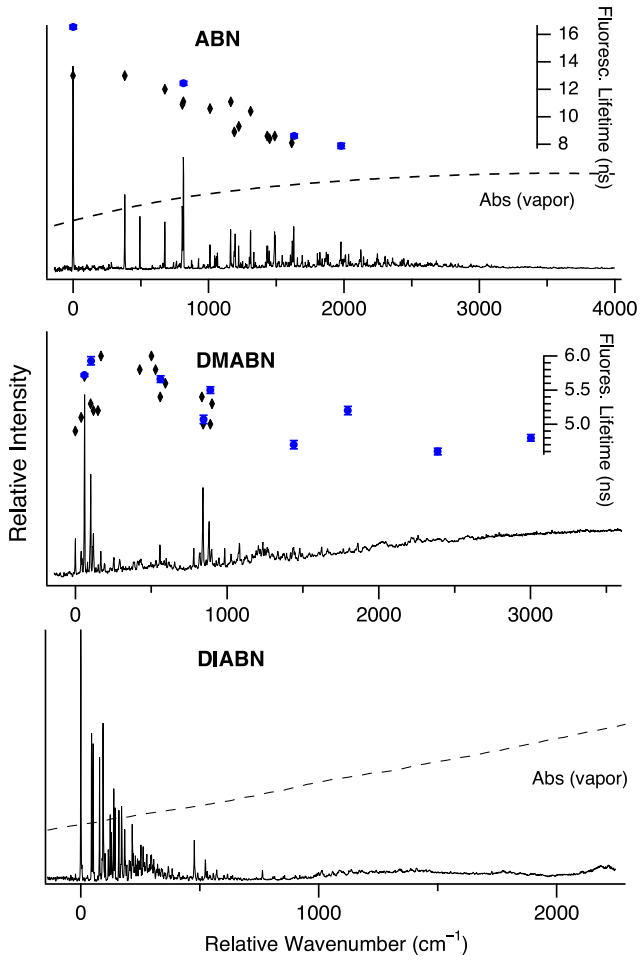

Fig. 11. Normalized fluorescence excitation spectra of 4-ABN, 4-DMABN, and 4-DIABN in a supersonic free jet. The excess energies are with respect to their origin bands. Inset plots represent the fluorescence lifetimes (in ns), measured as a function of the S_1 excess vibrational energy. Vapor-phase absorption spectra of 4-ABN and 4-DIABN are also shown (dashed curves). (Reprinted with permission from Ref. [59].)

the observation of an abrupt break-off (loss) of the LE fluorescence following higher-energy excitation of several aminobenzonitriles in the gas phase [59], Fig. 11, and the thermally activated $S_1(L_b) \rightarrow S_0$ internal conversion in alkane solvents [60], where no ICT reaction occurs. The observed threshold energy for fluorescence break-off, and the activation energy for internal conversion, are similar to the calculated energy barriers for the $\pi\pi^* \rightarrow \pi\sigma^*$ state switch [59].

Our calculations predict only one strongly allowed electronic transition from the lowest $\pi\sigma^*$ state to a higher state of the same nature [61]. For 4-DMABN, it is calculated at *ca.* 700 nm, Fig. 10 and Table 2. The excited-state transition absorptions from the $\pi\pi^*$ state (L_b or L_a) are much weaker. The calculation also indicates that the $\pi\sigma^*$ state can be identified by its anomalously low frequency ($\sim$1460 cm^{-1}) of the C–N stretch, relative to the corresponding vibrational frequencies ($\sim$2180 cm^{-1}) in the $\pi\pi^*$ and ground states [62]. The greatly reduced C–N stretch frequency of the $\pi\sigma^*$ state is due to the decrease in C–N bond order (from three to about two) that accompanies the $\pi \rightarrow \sigma^*$ excitation. Consistent with these predictions, 4-DMABN and 4-(diisopropylamino)benzonitrile (4-DIABN) display picosecond transient absorption at about 700 nm in non-polar and polar solvents following the 267 or 305 nm excitations of the L_a state [53,54]. Moreover, in 4-DMABN, the Raman active 1467 cm^{-1} C–N stretch exhibits a large resonance enhancement when the probe (Raman excitation) wavelength is set to near the spectral region of the $\pi\sigma^* \leftarrow \pi\sigma^*$ absorption at 600 nm and a decrease in intensity when the probe wavelength is set to 460 nm, where the $\pi\pi^* \leftarrow \pi\pi^*$ absorption occurs [62], Table 2. These results corroborate the existence of a low-ling $\pi\sigma^*$ state and the occurrence of an ultrafast (<1 ps) state switch from the initially excited $\pi\pi^*$ state (L_b or L_a) to the $\pi\sigma^*$ state.

We have proposed [58,61] that the highly polar $\pi\sigma^*$ state, which has a large dipole moment, is the intermediate state of the sequential ICT reaction that takes the initially excited $\pi\pi^*$ state to the fully charge-separated ICT state in 4-DMABN, Fig. 12. Consistent with this proposal, we have found that the ps rise time of the benzonitrile-anion-like ICT-state absorption at 410 nm is identical to the decay time of the $\pi\sigma^*$-state picosecond transient at 700 nm for 4-DMABN and 4-diisopropylaminobenzonitrile (4-DIABN) in acetonitrile [54], Fig. 13. The decay time and the rise time are significantly faster in 4-DIABN (<1 ps) than in 4-DMABN ($\sim$4 ps). Extension of the experimental and theoretical studies to other dialkylaminobenzonitriles and 4-(dimethylamino)phenylacetylene (4-DMAPA), shows that 2-DMABN and 3-DMABN, which possess high-lying $\pi\sigma^*$ state (relative to the initially excited $\pi\pi^*$ state), do not exhibit the 700 nm transient or the ICT reaction [54]. For molecules with the $^1\pi\sigma^*$ state below the low-lying $^1\pi\pi^*$ states, the lifetime of the 700 nm transient was found to be very short (a few picoseconds or less) for molecules that exhibit ICT, and very long (a few nanoseconds) for those that do not (e.g., 4-ABN and 4-DMAPA) [54]. These results corroborates the identification of the 700 nm transient as the $\pi\sigma^* \leftarrow \pi\sigma^*$ absorption and the important role the $\pi\sigma^*$ state plays in the ICT reaction of the EDA molecules.

Table 2
Comparison of TDDFT BP86/cc-pVDZ vertical excitation energies (in wavelengths) and oscillator strengths, *f*, of the lowest-energy $\pi\pi^*$ (L_b) and the lowest-energy $\pi\sigma^*$ singlet states of 4-DMABN with experimental transient absorptions in the visible region (400–700 nm)

Transition	λ_{calc}[a] (nm)	λ_{obs}[b] (nm)	f_{calc}[c]
$\pi\sigma^* \leftarrow \pi\sigma^*$	640	700	0.55 (0.50)
$\pi\pi^* \leftarrow \pi\pi^*$	524	525	0.07 (0.08)
$\pi\pi^* \leftarrow \pi\pi^*$	423	450	0.08 (0.14)

Reprinted with permission from Ref. [61].
[a] Only transitions with $f > 0.07$ are listed.
[b] From Ref. [44].
[c] The number in parenthesis represents the momentum representation transition moment.

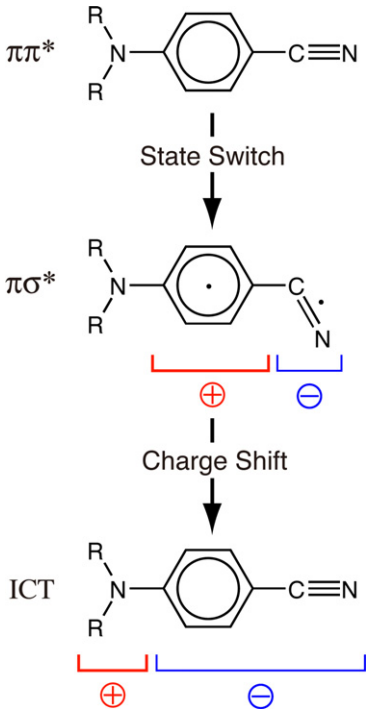

Fig. 12. Schematic mechanism for the $\pi\sigma^*$ state-mediated intramolecular charge transfer.

4. Assessment of computational methods

The theoretical support for the CI-mediated excited-state dynamics, described above, came from coupled-cluster (CC) and time-dependent DFT (TDDFT) methods of black box-type calculations. A reliable treatment of potential energy surfaces of excited states, including CI, requires methods that are able to include static (non-dynamical) and dynamic effects of electron correlation. This makes it necessary to utilize high-level ab initio methods such as multi-reference configuration interaction (MRCI) and complete active space plus perturbation theory in second order (CASPT2) [63]. In the latter approach, the CASSCF method is employed to define multi-references and add dynamical correlation through the use of the perturbation theory. Although CASPT2 and MRCI are undoubtedly the most accurate computational approaches currently available, they have limitations for the size of the molecules we have dealt with. Thus, the laborious CASPT2 method may encounter problems on the selection of CAS space and difficulties with balancing dynamical and non-dynamical correlation effects, while the more robust MRCI approaches are often prohibitively expensive. The usual CASPT2 method could, in fact, be just as incapable of describing conical interactions as much less expensive single reference methods. Only the multi-state variants of CASPT2 are expected to be capable of describing the intersections correctly. For excited states dominated by one-electron transitions, the standard CC and TDDFT methods appear to provide a good compromise between the accuracy and computational cost. They reproduce most of the important qualitative features of the excited-state dynamics of nucleic acid bases and 4-DMABN and related EDA molecules, as demonstrated in the previous two sections. Perhaps the most serious limitation of TDDFT is that it underestimates the excitation

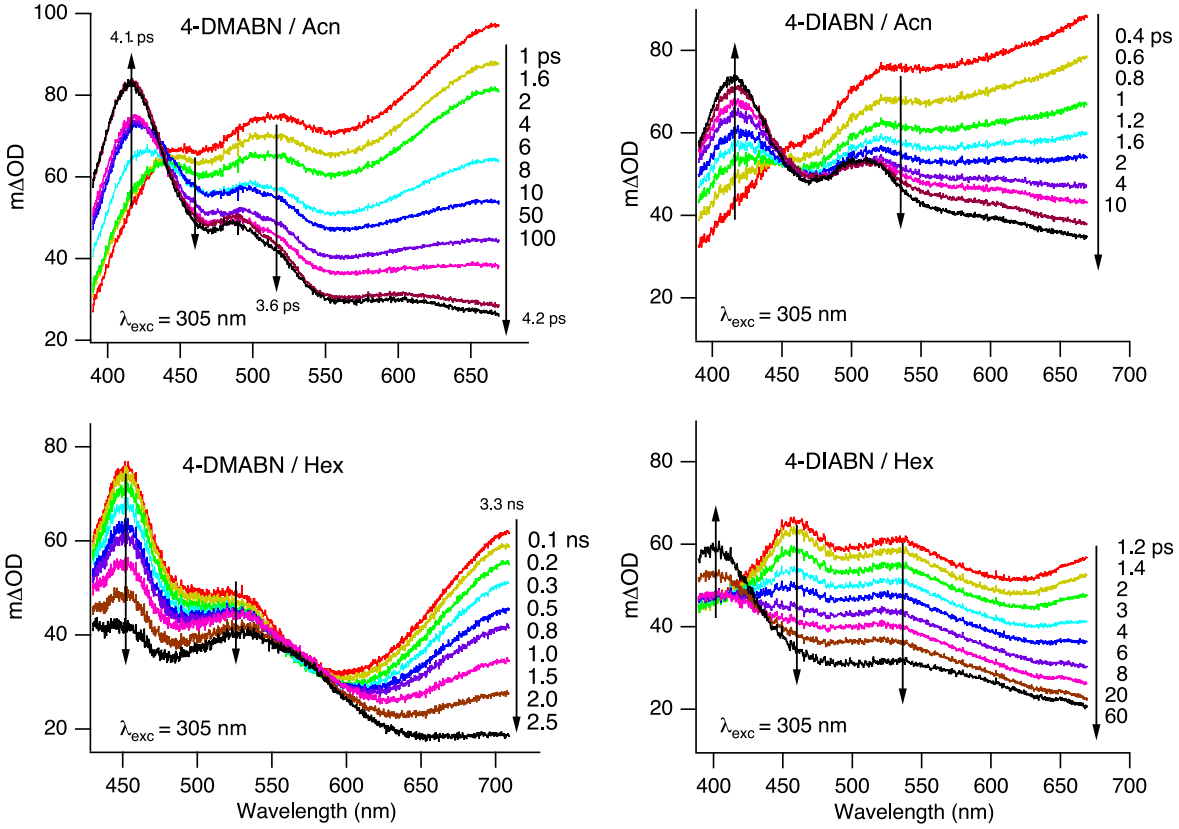

Fig. 13. Time-resolved transient absorption spectra for 4-DMABN (left panels) and 4-DIABN (right panels) in acetonitrile (Acn) and *n*-hexane (Hex) at room temperature. The arrows indicate time evolution (rise and decay) of the spectrum. (Reprinted with permission from Ref. [54].)

Table 3
Comparison of TDDFT adiabatic excitation energies (in eV) of 4-DMABN with CASPT2 calculations and experiment

State	Experiment[a]	CASPT2(10,9)[b]	CASPT2(12,12)[c]	B3LYP[d]	B-P[d]
$1\,^1B_2$ (LE, L_b)	4.02[e]	4.05	3.99	4.28	3.91
$2\,^1A_1$ (L_a)	<4.56[f]	4.41	4.39	4.50	4.13
$1\,^1A_2$ ($\pi\sigma^*$)	<4.09[g]		4.50 (15.5 D)[h]	4.20 (14.9 D)	3.47 (16.7 D)
TICT		3.94 (15.6 D)[f]	3.72 (15.0 D)[h]	3.46 (15.4 D)	2.59 (15.9 D)

Computed dipole moments of the $\pi\sigma^*$ and TICT states are given in parenthesis.
[a] In gas phase.
[b] Ref. [68] (for wagging angle of 0°).
[c] Ref. [69].
[d] Ref. [54].
[e] 0–0 Transition energy in a free jet (Ref. [59]).
[f] Vertical transition energy from electron energy loss spectra (Ref. [70]).
[g] Onset of fluorescence break-off in a free jet (Ref. [59]).
[h] Ref. [55].

energies of electronic states that have substantial charge transfer character [64,65]. This limitation, arising from self-interaction [66], can however be corrected in part by the use of a hybrid exchange correlation functional, such as B3LYP, as illustrated in Table 3. As for CC, the standard methods, such as CC2 and equation of motion coupled-cluster (EOM-CCSD), appear to work well for excited states dominated by single excitation from the ground state. For degenerate or quasi-degenerate systems and excited states dominated by double excitation from the ground state, biradicals, and other open-shell systems, renormalized coupled-cluster methods are available [67]. For the small diatomic and triatomic molecules, this relatively inexpensive black-box CR-EOM-CCSD(T) approach has proven to provide energies of excited electronic states (dominated by two-electron excitations) with accuracies on the order of 0.1 eV. In our own work on nucleobases (adenine, for example), CR-EOM-CCSD(T) yields excited-state energies and state ordering ($n\pi^*$ and $\pi\pi^*$) that are in reasonable agreement with those from CASPT2//CASSCF calculations, as shown in Table 4.

To summarize, the computationally straightforward, and inexpensive, methods utilized in this work appear to provide all essential qualitative features of the experimental observation pertaining to the excited-state dynamics that occur via three-state conical intersections. This is fortunate, since the simplicity of computational methods is important, if not essential, in investigating excited states of larger biomolecules, including fragments of DNA chain. Nonetheless, it would be prudent to check the reliability of the results from the low-level calculations by single-point energy calculations based on much higher levels of theory.

Table 4
Comparison of CR-EOM-CCSD(T) vertical excitation energies (in eV) of adenine with the results from CASPT2//CASSCF calculations

State	CASPT2[a]	CASPT2[b]	CASPT2[c]	CR-EOM-CCSD(T)[d]
$\pi\pi^*$	4.74	4.96	5.01	4.90
$n\pi^*$	5.00	5.16	5.05	4.94

[a] Ref. [71].
[b] Ref. [41].
[c] Ref. [72].
[d] Ref. [32].

Acknowledgments

We are grateful to the U.S. Department of Energy and Ohio Supercomputer Center for the financial support, and to Drs. Ricardo Campos Ramos, Jae-Kwang Lee, William G. Kofron, and Serguei Patchkovskii for their contributions to the work described in this Letter.

References

[1] E. Teller, J. Phys. Chem. 41 (1937) 109.
[2] M. Klessinger, J. Michl, Excited States and Photochemistry of Organic Molecules, VCH, New York, 1995.
[3] M.A. Robb, F. Bernardi, M. Olivucci, Pure Appl. Chem. 67 (1995) 783.
[4] D.R. Yarkony, Rev. Mod. Phys. 68 (1996) 985.
[5] W. Domcke, G. Stock, Adv. Chem. Phys. 100 (1997) 1.
[6] K. Andersson, P.A. Malmqvist, B.O. Roos, J. Chem. Phys. 96 (1992) 1218.
[7] J.J.W. McDouall, K. Peasley, M.A. Robb, Chem. Phys. Lett. 148 (1988) 183.
[8] J. Finley, P.-A. Malmqvist, B.O. Roos, L. Serrano-Andres, Chem. Phys. Lett. 288 (1998) 299.
[9] D. Zhong, E.W.G. Diau, T.M. Bernhardt, S. De Feyter, J.D. Roberts, A.H. Zewail, Chem. Phys. Lett. 298 (1998) 129.
[10] E.W.G. Diau, S. De Feyter, A.H. Zewail, J. Chem. Phys. 110 (1999) 9785.
[11] J.-M.L. Pecourt, J. Peon, B. Kohler, J. Am. Chem. Soc. 122 (2000) 9348.
[12] J. Peon, A.H. Zewail, Chem. Phys. Lett. 348 (2001) 255.
[13] See, for a recent review: C.E. Crespo-Hernandez, B. Cohen, P.M. Hare, B. Kohler, Chem. Rev. 104 (2004) 1977.
[14] See, for a recent review: Z.R. Grabowski, K. Rotkiewicz, W. Rettig, Chem. Rev. 103 (2003) 3899.
[15] M.Z. Zgierski, T. Fujiwara, E.C. Lim, in: M. Shulkla, J. Leszczynski (Eds.), Radiation Induced Molecular Phenomena in Nucleic Acids, Springer, New York, 2008.
[16] B.R. Henry, W. Siebrand, Organic Moleclar Potophysics, Wiley Interscience, London, 1970.
[17] K.F. Freed, in: F.K. Fong (Ed.), Topics in Applied Physics, Springer, Berlin, 1976, p. 23.
[18] P. Avouris, W.M. Gelbart, M.A. El-Sayed, Chem. Rev. 77 (1977) 793.
[19] E.C. Lim, Advances in Photochemistry 23 (1997) 165.
[20] J. Eisinger, A.A. Lambola, in: R.F. Steiner, I. Weinryb (Eds.), Excited States of Proteins and Nucleic Acids, Plenum Press, New York, 1971, p. 107.
[21] N.J. Kim, G. Jeong, Y.S. Kim, J. Sung, S. Keun Kim, Y.D. Park, J. Chem. Phys. 113 (2000) 10051.
[22] E. Nir, K. Kleinermanns, L. Grace, M.S. de Vries, J. Phys. Chem. A 105 (2001) 5106.
[23] M.Z. Zgierski, S. Patchkovskii, E.C. Lim, J. Chem. Phys. 123 (2005) 081101.
[24] M.Z. Zgierski, S. Patchkovskii, E.C. Lim (2005), unpublished results.
[25] M.Z. Zgierski, S. Patchkovskii, T. Fujiwara, E.C. Lim, J. Phys. Chem. A 109 (2005) 9384.
[26] L. Blancafort, B. Cohen, P.M. Hare, B. Kohler, M.A. Robb, J. Phys. Chem. A 109 (2005) 4431.
[27] R.J. Malone, A.M. Miller, B. Kohler, Photochem. Photobiol. 77 (2003) 158.
[28] T. Fujiwara, E.C. Lim, 2006, unpublished results based on fluorescence decay measurement.
[29] M.Z. Zgierski, T. Fujiwara, W.G. Kofron, E.C. Lim, Phys. Chem. Chem. Phys. 9 (2007).
[30] B. Cohen, C.E. Cespo-Hernandez, B. Kohler, Faraday Disucss. 127 (2004) 137.
[31] T. Gustavsson et al., J. Am. Chem. Soc. 128 (2006) 607.
[32] M.Z. Zgierski, S. Patchkovskii, E.C. Lim, Can. J. Chem. 85 (2007) 124.
[33] M.Z. Zgierski, S. Patchkovskii, T. Fujiwara, E.C. Lim, 2006, unpublished results.
[34] C. Canuel, M. Mons, F. Piuzzi, B. Tardivel, I. Dimicoli, M. Elhanine, J. Chem. Phys. 122 (2005) 074316.
[35] K. Tomic, J. Tatchen, C.M. Marian, J. Phys. Chem. A 109 (2005) 8410.
[36] S. Matsika, J. Phys. Chem. A 108 (2004) 7584.
[37] S. Perun, A.L. Sobolewski, W. Domcke, J. Phys. Chem. A 110 (2006) 13238.
[38] H. Chen, S. Li, J. Chem. Phys. 124 (2006) 154315.
[39] C.M. Marian, J. Chem. Phys. 122 (2005) 104314.
[40] S. Perun, A.L. Sobolewski, W. Domcke, J. Am. Chem. Soc. 127 (2005) 6257.
[41] L. Serrano-Andres, M. Merchan, A.C. Borin, Proc. Natl. Acad. Sci. USA 103 (2006) 8691.
[42] M.Z. Zgierski, S. Patchkovskii, T. Fujiwara, E.C. Lim, Chem. Phys. Lett. 440 (2007) 145.
[43] E. Lippert, W. Lüder, H. Boos, Advances in Molecular Spectroscopy, Pergamon, Oxford, 1962.
[44] T. Okada, N. Mataga, W. Baumann, J. Phys. Chem. 91 (1987) 760.
[45] K. Rotkiewicz, Chem. Phys. Lett. 19 (1973) 315.
[46] Z.R. Grabowski, K. Rotkiewicz, A. Siemiarczuk, D.J. Cowley, W. Baumann, Nouv. J. Chim. 3 (1979) 443.
[47] W. Rettig, Angew. Chem. 25 (1986) 971.
[48] Y.V. Il'ichev, W. Kuehnle, K.A. Zachariasse, J. Phys. Chem. A 102 (1998) 5670.
[49] K.A. Zachariasse, Chem. Phys. Lett. 320 (2000) 8.
[50] For a comprehensive listing of theoretical work, see A. Köhn, C. Hättig, J. Am. Chem. Soc. 126 (2004) 7399, and earlier references therein.
[51] W.M. Kwok et al., J. Phys. Chem. B 105 (2001) 984.
[52] J. Dobkowski, J. Wojcik, W. Kowminski, R. Kolos, J. Waulk, J. Michl, J. Am. Chem. Soc. 124 (2002) 2406.
[53] S.I. Druzhinin, N.P. Ernsting, S.A. Kovalenko, L.P. Lustres, T.A. Senyushkina, K.A. Zachariasse, J. Phys. Chem. A 110 (2006) 2955.
[54] J.-K. Lee, T. Fujiwara, W.G. Kofron, M.Z. Zgierski, E.C. Lim, J. Chem. Phys. 128 (2008) 164512.
[55] A.L. Sobolewski, W. Sudholt, W. Domcke, J. Phys. Chem. A 102 (1998) 2716.
[56] A.L. Sobolewski, W. Domcke, Chem. Phys. Lett. 250 (1996) 428.
[57] A.L. Sobolewski, W. Domcke, Chem. Phys. Lett. 259 (1996) 119.
[58] M.Z. Zgierski, E.C. Lim, J. Chem. Phys. 121 (2004) 2462.
[59] R. Campos Ramos, T. Fujiwara, M.Z. Zgierski, E.C. Lim, J. Phys. Chem. A 109 (2005) 7121.
[60] S.I. Druzhinin, A. Demeter, V.A. Galievsky, T. Yoshihara, K.A. Zachariasse, J. Phys. Chem. A 107 (2003) 8075.
[61] M.Z. Zgierski, E.C. Lim, J. Chem. Phys. 122 (2005) 111103.
[62] C. Ma, W.M. Kwok, P. Matousek, A.W. Parker, D. Phillips, W.T. Toner, M. Towrie, J. Phys. Chem. A 106 (2002) 3294.
[63] M. Merchan, L. Serrano-Andres, Theor. Comput. Chem. 16 (2005) 35.
[64] M.E. Casida, F. Gutierrez, J. Guan, F.-X. Gadea, D. Salahub, J.-P. Daudey, J. Chem. Phys. 113 (2000) 7062.
[65] A. Dreuw, J.L. Weisman, M. Head-Gordon, J. Chem. Phys. 119 (2003) 2943.
[66] J.P. Perdew, A. Zunger, Phys. Rev. B 23 (1981) 5048.
[67] P. Piecuch, K. Kowalski, I.S.O. Pimienta, M.J. McGuire, Int. Rev. Phys. Chem. 21 (2002) 527.
[68] L. Serrano-Andres, M. Merchan, B.O. Roos, R. Lindh, J. Am. Chem. Soc. 117 (1995) 3189.
[69] W. Sudholt, A. Staib, A.L. Sobolewski, W. Domcke, Phys. Chem. Chem. Phys. 2 (2000) 4341.
[70] C. Bulliard, M. Allan, G. Wirtz, E. Haselbach, K.A. Zachariasse, N. Detzer, S. Grimme, J. Phys. Chem. A 103 (1999) 7766.
[71] H. Chen, S. Li, J. Phys. Chem. A 109 (2005) 8443.
[72] L. Blancafort, J. Am. Chem. Soc. 128 (2006) 210.

Marek Z. Zgierski received his Ph.D. in 1971 and D.Sc in 1976 from the Jagiellonian University in Kracow, Poland. In 1977, he joined National Research Council of Canada in Ottawa, where he is a Senior Research Officer. His primary scientific interests are radiationless transitions and manifestation of vibronic coupling in various branches of spectroscopy of polyatomic molecules.

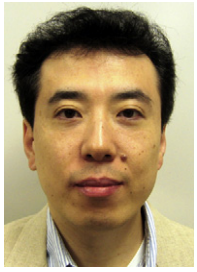

Takashige Fujiwara is a senior research associate at The University of Akron. He received his M.S. (1993) and Ph.D. (2000) from Kyoto University, Japan. His primary research interests are laser spectroscopy and molecular photophysics.

Edward C. Lim (Ph.D., Oklahoma State, 1959) is the holder of the Goodyear Chair, and the Director of the Center for Laser and Optical Spectroscopy, at The University of Akron. His principal research interests are in the area of electronic spectroscopy and photophysics of organic molecules, with recent efforts focused on the low-lying dark electronic state and the role they play in ultrafast excited-states dynamics.